Available online at www.sciencedirect.com

SciVerse ScienceDirect

Journal of the European Ceramic Society 32 (2012) 1733–1741

www.elsevier.com/locate/jeurceramsoc

Thin film yttria-stabilized zirconia electrolyte for intermediate-temperature solid oxide fuel cells (IT-SOFCs) by chemical solution deposition

Eun-Ok Oh [a,c], Chin-Myung Whang [a], Yu-Ri Lee [b,c], Jong-Heun Lee [b], Kyung Joong Yoon [c], Byung-Kook Kim [c], Ji-Won Son [c], Jong-Ho Lee [c], Hae-Weon Lee [c,*]

[a] *School of Materials Science and Engineering, and Institute of Advanced Materials, Inha University, 253 Youghyun, Incheon 402-751, South Korea*
[b] *Materials Science and Engineering, Korea University, Anam, Seongbuk, Seoul 136-701, South Korea*
[c] *High Temperature Energy Materials Center, Korea Institute of Science and, Technology, 39-1 Hawolgok, Seongbuk, Seoul 136-791, South Korea*

Received 9 August 2011; received in revised form 11 January 2012; accepted 18 January 2012
Available online 14 February 2012

Abstract

A 500 nm thick thin film YSZ (yttria-stabilized zirconia) electrolyte was successfully fabricated on a conventionally processed anode substrate by spin coating of chemical solution containing slow-sintering YSZ nanoparticles with the particle size of 20 nm and subsequent sintering at 1100 °C. Incorporation of YSZ nanoparticles was effective for suppressing the differential densification of ultrafine precursor powder by mitigating the prevailing bi-axial constraining stress of the rigid substrate with numerous local multi-axial stress fields around them. In particular, adding 5 vol% YSZ nanoparticles resulted in a dense and uniform thin film electrolyte with narrow grain size distribution, and fine residual pores in isolated state. The thin film YSZ electrolyte placed on a rigid anode substrate with the GDC (gadolinia-doped ceria) and LSC ($La_{0.6}Sr_{0.4}CoO_{3-\delta}$) layers deposited by PLD (pulsed laser deposition) processes revealed that it had fairly good gas tightness relevant to a SOFC (solid oxide fuel cell) electrolyte and maintained its structural integrity during fabrication and operation processes. In fact, the open circuit voltage was 1.07 V and maximum power density was 425 mW/cm^2 at 600 °C, which demonstrates that the chemical solution route can be a viable means for reducing electrolyte thickness for low- to intermediate-temperature SOFCs.

Keywords: Sol–gel processes; Microstructure; Fuel cells; Y_2O_3–ZrO_2; Constrain sintering

1. Introduction

There has been a great deal of interest in producing thin-film electrolytes by chemical solution techniques[1,2] for the purpose of operating solid oxide fuel cell (SOFC) at lower temperatures.[3–6] avoiding electrolyte leakage[7–9] and applying a diffusion barrier layer. [10,11] In general, the chemical solution techniques have been considered to be inexpensive in terms of initial capital investment and simple in principle like the conventional processes. In addition, once the precursor chemistry and processing conditions are optimized, they can be readily applied to the substrates of large area without delicate process adjustments. Despite many technical advantages, the application of chemical solution route in SOFCs has been very limited in practice because the preparation of thin films by chemical solution deposition requires careful optimization of individual process steps including dispersion, coating, drying, and sintering.

The chemical solution deposition techniques for thin film preparation can be divided into two categories depending on the delivery of chemical solution to the substrate to be coated. Some techniques, such as dip coating and spin coating, transfer the bulk solution onto the substrate to be dried as a whole,[1–6] while the other techniques, including electrostatic spray deposition (ESD) and inkjet printing, transfer the chemical solution in the form of droplets to be coalesced and dried on the substrate.[8–10] Although all of them can be applied to produce gastight thin films of relatively high density with optimized film thickness, the difference in the solution delivery and its effect on drying leads to substantial variations of microstructural heterogeneities and film thickness required for gas tightness. For example, multiple coating practice in dip coating and spin coating generates microstructural heterogeneities between the individual sub-layers, and the droplet delivery in ESD and inkjet printing commonly suffers from the incomplete coalescence of the

* Corresponding author. Tel.: +82 2 958 5523, fax: +82 2 958 5529.
E-mail addresses: hwlee@kist.re.kr, sofc.lee@gmail.com (H.-W. Lee).

0955-2219/$ – see front matter © 2012 Elsevier Ltd. All rights reserved.
doi:10.1016/j.jeurceramsoc.2012.01.021

droplets. These microstructural heterogeneities are dependent upon the delivery method and drying mechanisms of chemical solution deposition techniques.

In addition, the process optimization becomes even more complicated when the substrates to be coated do not possess the adequate surface quality for chemical solution deposition of thin film, like the porous anode substrates of anode-supported SOFCs.[12–18] If the thin film is deposited and sintered on a rigid substrate by a chemical solution method, the process shrinkages associated with drying and sintering will generate substantial mismatch strains and cause a wide spectrum of microstructural heterogeneities.[12,19–24] The microstructural heterogeneities formed in chemical solution deposition can grow to macro-scale process flaws during drying and sintering in the presence of the constraining stresses generated by the non-sintering substrate. The occurrence of microstructural heterogeneities will be even more pronounced in the coating layer which is composed of ultrafine sol particles of extremely fast sintering rate typically derived from chemical solutions. According to the previous investigations,[4,6,7] they often reported that there were less dense boundaries between the sub-layers of the thin film due to the inhomogeneous packing which originated from multiple coating practice frequently employed for increasing the film thickness to a desired level. The inhomogeneous packing commonly led to differential sintering which resulted in considerable retardation of overall densification and relatively high residual porosity with pore anisotropy. Especially when the coating layer is composed of extremely fine sol particles of fast sintering rate, even small microstructural heterogeneities can grow to put the structural integrity of the thin films in danger. In an extreme case, the substantially high mismatch strain generated by fast-sintering sol particles causes a thin film to completely peel off from a rigid substrate since the thin film undertakes extensive densification prior to developing its adhesion to the substrate.

Therefore, it is essential to decrease the sintering rate of the sol particles in the thin film produced by chemical solution deposition in order to allow it to develop sufficient adhesion strength to the substrate. In the present study, slow-sintering YSZ nanoparticles are incorporated into the chemical solution and consequently into the precursor powders which undergo constrained sintering at reduced densification rate under the multiaxial stress fields of substantially smaller magnitude than the substrate constraint.[20–24] A cell comprising a thin film YSZ electrolyte was fabricated on a rigid anode substrate by multiple spin coating of chemical solution with YSZ nanoparticle addition and by placing both the gadolinia-doped ceria (GDC) barrier and $La_{0.6}Sr_{0.4}CoO_3$ (LSC) cathode layers via pulsed laser deposition (PLD) process, and the feasibility of a thin film YSZ electrolyte was evaluated for its application to the SOFC operating at low to intermediate temperatures.

2. Experimental procedures

Zirconium acetate in acetic acid in a solution (Aldrich, USA) and yttrium nitrate hexahydrate (Aldrich, USA) were used as starting precursors for the preparation of an 8 mol% yttria stabilized zirconia (8YSZ) solution. Dimethylformamide (DMF, Aldrich, USA) was used as the solvent, which also acted as a drying control chemical additives (DCCA). Ethanol (EtOH, Aldrich, USA) was also used as a co-solvent and acetylacetone (Acac, Aldrich, USA) was used as a complexing agent. The molar ratio of DMF:EtOH:H_2O:Acac mixed solution was 1.4:0.62:0.5:0.27 and the YSZ precursors were added in the mixed solution. The prepared YSZ solution was stirred for 6 h and evaporated to 2 M. The pH value of the solution was measured to be around 4. A solution containing nanoparticles was prepared by adding 8YSZ nanoparticles (Nextech, USA) into the above 8YSZ solution. The primary particle size and surface area of the YSZ nanoparticles were 20 nm and 155 m^2/g, respectively. Content of YSZ nanoparticles (YSZ-NP) was varied from 1 to 9 vol% based on the final YSZ yield. Polyvinylpyrrolidone (PVP, $M_n = 10{,}000$, Aldrich, USA), which is a non-ionic polymer with excellent solubility in both alcohol and water, was added as a dispersion agent at 25 wt% based on a dry weight of incorporated YSZ nanoparticles. With this non-ionic nature of PVP, it can stabilize the YSZ nanoparticle via steric stabilization mechanism. Intensive ultrasonication treatment was applied for 3–5 h depending on the content of the added YSZ nanoparticles to prepare stable nanoparticle-dispersed solutions.

The chemical solution deposition was carried out by spin coating on both the dense sapphire and porous NiO–YSZ substrates[25] at a rotation speed of 2000 rpm for 60 s using a spin-coater (JSP4D, JD Tech, Korea). The thickness after each spin coating was in the range of 80–100 nm depending on the content of YSZ nanoparticles. After each spin coating, the film was dried by heating in a microwave oven at 200 °C in flowing air condition to remove gaseous species coming out from the sample, and the processing steps of spin coating and microwave drying were repeated until the electrolyte films thickness approached to the desired one, e.g. 400–500 nm. The sintering was carried out by heating to 1100 °C without holding time followed by reducing to 1000 °C and holding for 12 h. The heating rate was varied from 0.25 to 1 °C/min. For the evaluation of YSZ thin film as an electrolyte of SOFC, a cell was fabricated by applying GDC interdiffusion barrier and LSC cathode layers by PLD process.

Film thickness and microstructure of the YSZ thin films were investigated using scanning electron microscope (SEM, FEI XL-30 FEG) and field emission gun transmission electron microscope (FE-TEM, Tecnai G2, USA). The cell containing YSZ thin film electrolyte was evaluated in terms of *I–V–P* characteristics at 450–600 °C using electrochemical interface analyzer (Solartron 1287, AMETEK, UK).

3. Results and discussion

SEM micrographs in Fig. 1 show critical process flaws which are commonly observed in fabricating a thin film YSZ electrolyte on a rigid substrate by chemical solution deposition method. Large surface cracks in Fig. 1(a) usually originate from microcracks by differential drying and subsequently grow to macrocracks by differential sintering. In general, chemical solution route always suffers from extremely large process shrinkage and poor packing homogeneity regardless of deposition

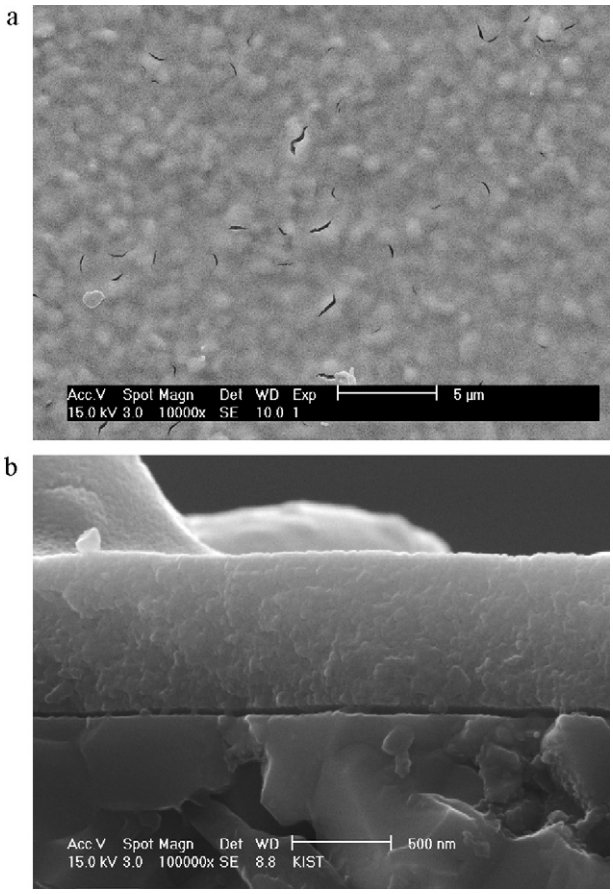

Fig. 1. SEM micrographs of critical process flaws observed in a thin film YSZ electrolyte prepared by chemical solution deposition method: (a) surface cracks and (b) delamination crack.

techniques since the chemical solution contains very large amount of solvent and organic additives. Thus even small microstructural heterogeneities produced in the film deposition step are detrimental to the structural integrity of the thin film, since the transient stress, arising from differential densification in the presence of non-sintering substrate, can cause them to grow to macrocracks to structural damages. Given that the differential densification originates from the difference of the densification rate between the local areas inside the thin film, the magnitude of transient stress is dependent mainly on the intrinsic densification rate of the precursor powder relative to the non-sintering substrate. Considering the ultrafine nature of the precursor powder obtained from the chemical solution, it is its intrinsic densification rate that does control the magnitude of the transient stress with other factors kept constant. Therefore, it is essential to control the densification behavior of the precursor powder in order to prevent the ever-present microstructural heterogeneities from growing to large process flaws.

Another serious flaw is a delamination crack between the substrate and thin film electrolyte, as shown in Fig. 1(b). This delamination crack can be attributed to the intrinsically fast densification rate of the precursor powder in the thin film on the non-sintering substrate. When a thin film, deposited on a rigid substrate by chemical solution, undergoes sintering, there occur two concurrent events of the densification of thin film itself and its adhesion to the substrate. If the densification rate of the thin film is faster than the development rate of its adhesion to the substrate, the delamination cracks are readily generated as shown in Fig. 1(b). In an extreme case, thin film electrolyte layer can be completely peeled off from the substrate with the substrate surface exposed to the open air. This discloses that the generation of delamination cracks can be attributed to the rapid densification rate of the ultrafine precursor powder obtained from chemical solution on a rigid substrate.

Since the mismatch strain in this case is exactly equivalent to the process shrinkage of the thin film itself, due attention should be paid to both the drying and binder burn-out steps in which substantially large shrinkages lead the thin film to various microstructural heterogeneities such as microcracks, large pores and inhomogeneous packing. When microstructural heterogeneities are produced in the early process steps, they are likely to grow to critical process flaws in the subsequent sintering step. Since the transient stresses generated by differential densification are unavoidable during sintering of a thin film on a rigid substrate, it is very important to relieve or reduce them in order to avoid the generation of critical process flaws. A conventional attempt was made to accomplish this by incorporating slow-sintering YSZ nanoparticles into the precursor powder matrix, i.e. chemical solution. Uniformly dispersed YSZ nanoparticles will generate constraining stress fields around them in the precursor powder matrix, which is expected to change the prevailing bi-axial stress field by the rigid substrate to multi-axial stress fields of considerably small magnitudes. These multi-axial stress fields may force the precursor powder particles to rearrange themselves for improving packing homogeneity, through which the drying stresses generated by the substantially large shrinkages associated with the removal of organic substances can be effectively relieved or reduced. Moreover, the local constraining effect of YSZ nanoparticles also contributes to reduced overall densification of the thin film YSZ electrolyte at high temperatures as long as there exists the difference of particle size, i.e. sintering rate, between the matrix particles and slow-sintering YSZ nanoparticles.

Although the shrinkage behavior of the thin film coating cannot be precisely measured, the green compacts prepared with the dried precursor powders may reflect the effect of the YSZ nanoparticles on the sintering of precursor powder matrix. Fig. 2 shows plots of linear shrinkages for the compacts prepared using the dried precursor powders with and without YSZ nanoparticles. As expected, the shrinkage behaviors are very similar and the total shrinkage approaches almost 35% corresponding to the packing density of about 27% under the assumption that the shrinkages are identical regardless of measurement directions. This reflects that the precursor powder compacts are composed of low-density aggregate network formed between very small particles precipitated from the ionic solutions. Judging from XRD analysis and TEM observation, the crystallite size was only 5 nm even after heat treatment at 600 °C which is substantially smaller than the primary particle size of YSZ nanopowder incorporated into the precursor solutions. Since the majority of sintering shrinkage takes place in the range 300–600 °C, the stress fields developed around the YSZ nanoparticles are

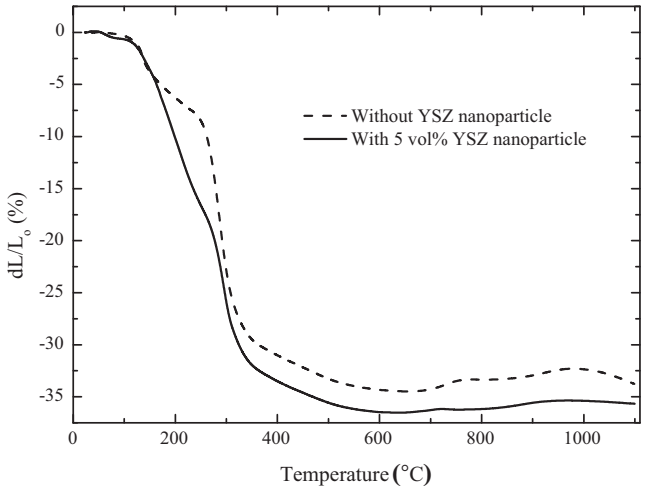

Fig. 2. Plots of sintering shrinkage as a function of temperature for the compacts prepared with the precursor powders with and without YSZ nanoparticle addition.

expected to force the extremely fine precursor powder particles to rearrange themselves for improved packing homogeneity. In consequence, the slightly increased shrinkage in the compact with YSZ nanoparticle addition should be attributed to the improved microstructural homogenization by particle rearrangement of precursor powder particles arising from the local stress fields generated around the uniformly dispersed YSZ nanoparticles.

In fact, SEM micrographs in Fig. 3 show the sintered surface of the thin film YSZ electrolytes deposited on sapphire substrates containing different amounts of slow-sintering YSZ nanoparticles, which were prepared by spin coating of corresponding chemical solutions and subsequent sintering. Regardless of the content of YSZ nanoparticles, there were no major process flaws except residual porosity and overall microstructure was relatively uniform throughout the YSZ electrolyte surfaces. For the thin film electrolytes containing 5 vol% YSZ nanoparticles or less, the pore size decreases with increasing the content of nanoparticles, while the grain size is the smallest for the thin film containing 2 vol% YSZ nanoparticles. Among them, the thin film electrolyte prepared with 5 vol% YSZ nanoparticles shows the most favorable microstructure with narrow grain size distribution and fine residual pores evenly distributed throughout the film. This supports the contention that local stress fields generated around the YSZ nanoparticles contribute to the microstructural homogenization by particle rearrangement and grain growth inhibition even in the presence of rigid substrate. In terms of microstructural homogenization, the optimum content of slow-sintering YSZ nanoparticles appears to be around 5 vol% based on total YSZ yield below which the magnitude of local stresses may not be large enough for mitigating the constraining stress of the rigid substrate. Based on the

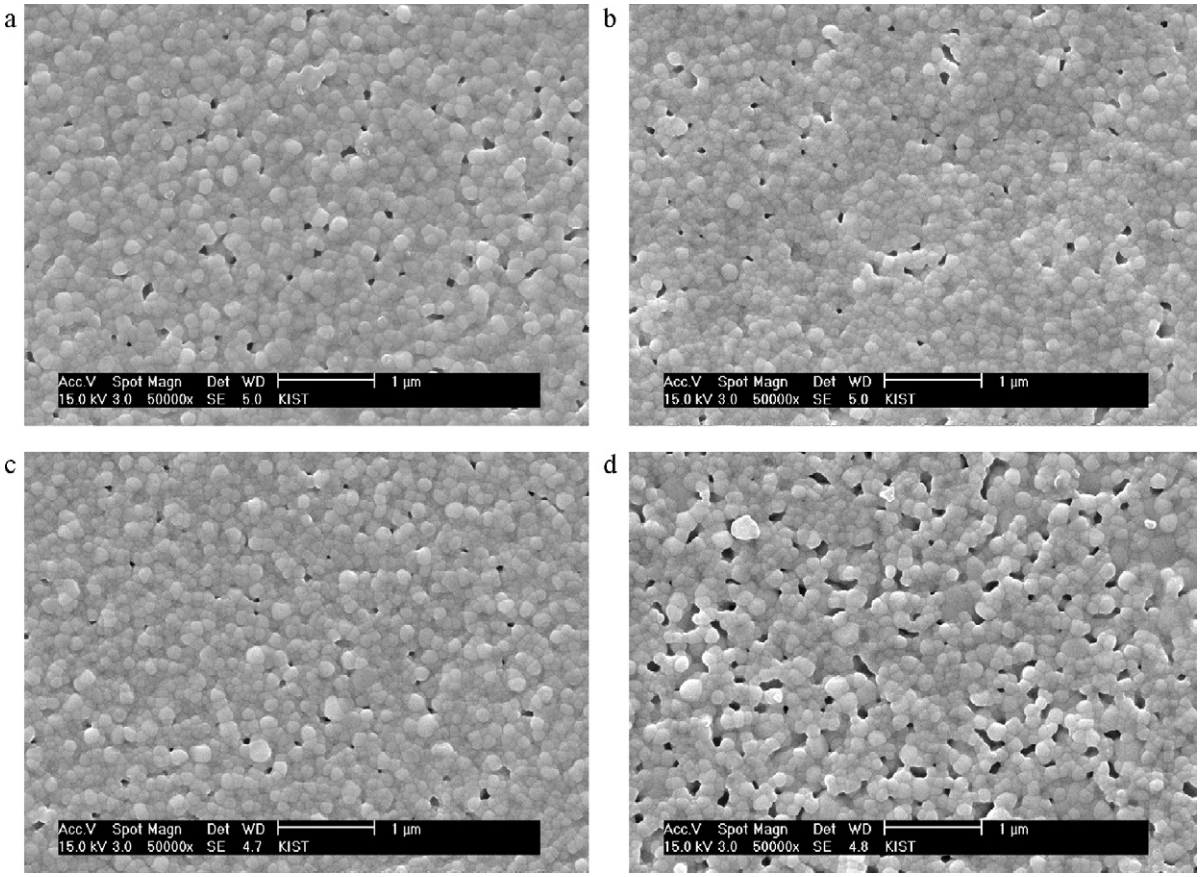

Fig. 3. SEM images showing the microstructures of the thin film YSZ electrolytes prepared with different amounts of slow-sintering YSZ nanoparticle addition based on total YSZ yield: (a) 1 vol%, (b) 2 vol%, (c) 5 vol% and 9 vol%.

aforementioned observation, it is suggested that controlling the magnitude of local constraints with the content of slow-sintering YSZ nanoparticles can be a practical means for improving microstructural homogeneity, reducing the degree of differential densification and eventually suppressing process flaws.

Unlike evenly distributed fine pores in the isolated state shown in Fig. 3(a)–(c), there are extensive interactions between the residual pores of relatively large sizes to form pore clusters for the thin film prepared with 9 vol% YSZ nanoparticle addition, as shown in Fig. 3(d). If the slow-sintering YSZ nanoparticles are added above a critical volume fraction, they undergo substantial interparticle interactions and eventually get into close contacts with each other to form local clusters. Once local clusters of slow-sintering particles are formed throughout the matrix, the densification of the precursor powder matrix nearly ceases until the slow-sintering particles themselves take part in sintering process at higher temperatures. The microstructure seen in Fig. 3(d) clearly shows that local clustering of slow-sintering particles is always accompanied by the appearance of large pores near and inside them since there is insufficient amount of precursor powder available for densification. Hence, it is necessary to carefully optimize the content of slow-sintering YSZ nanoparticles in order to avoid the formation of local clusters. According to previous investigations on the structural stability of thin film,[7,26] the breakup of thin film can take place when grain growth occurs to such an extent that grain size is greater than the film thickness. The grain sizes in Fig. 2 are in the range 30–100 nm which is much smaller than the film thickness of the electrolyte layer, e.g. 500 nm. This assures that the thin film YSZ electrolyte fabricated in this study can maintain its structural stability unless there is a drastic increase of grain size in the subsequent process steps.

TEM investigation of the cross sections provides more detailed information on the mictrostructure development of thin film YSZ electrolyte layer under the constrained sintering in the presence of the rigid substrate. Fig. 4 shows a cross section of sintered thin film YSZ electrolyte prepared by multiple spin coating and subsequent sintering. There are a couple of large pores located just underneath the surface region in combination with many small pores distributed throughout the thin film. The unusual morphological development of anisotropic pores has been observed repeatedly in the thin films prepared by multiple spin coating of chemical solutions. In order to elucidate their origins, the thin film electrolyte formed by multiple spin coating was partially sintered in both the resistive and microwave heating conditions and a comparison is made in terms of pore structure development. In doing so, microwave heating was intended for ruling out the additional constraining effect by the preferential densification of the surface region occurring in resistive heating, since it provides an ideal condition with volumetric heating for investigating the development of anisotropic pores between sub-layers. Fig. 5 shows TEM micrographs of the YSZ thin film electrolyte layers prepared by resistive heating (Fig. 5(a)) at 800 °C and microwave heating (Fig. 5(b)) at 800 °C. There are clearly several layers of dark regions separated by almost equally spaced bright bands which could be attributed to the presence of packing inhomogeneities in the sub-boundaries, as

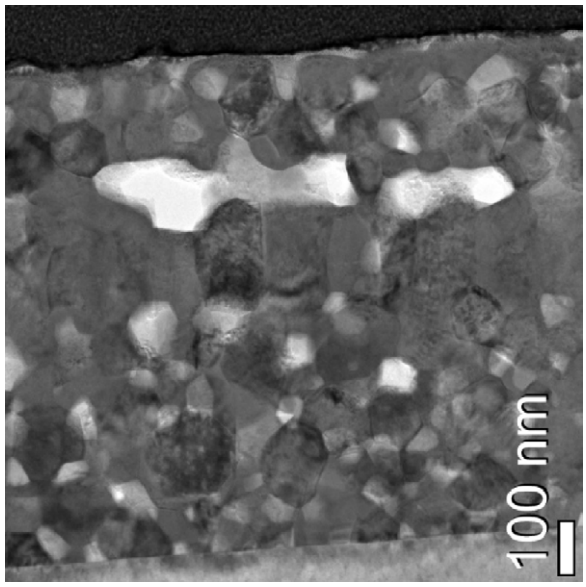

Fig. 4. TEM images of the cross sections of sintered thin film YSZ electrolyte showing elongated pores due to differential densification in the presence of packing inhomogeneity.

shown in Fig. 5(a). Once the thin film electrolyte layer formed by multiple spin coating was subjected to microwave sintering at 800 °C, the bright bands were enlarged due to the accelerated differential densification under fast heating condition, as shown in Fig. 5(b). This undoubtedly supports the fact that those pore clusters in Fig. 3 originate from the packing inhomogeneity formed during multiple spin coating and that they become more pronounced when the sintering condition is in favor of fast densification rate like microwave heating.

In several previous investigations,[7,9,15,18] the separation bands were also observed between the sub-layers of the thin films prepared by multiple coating of chemical solution, but it was postulated that the separation lines disappeared when it was sintered at higher temperatures. Those pore clusters can be readily produced in the presence of the packing non-uniformities when the sub-layers undergo extremely fast sintering rate at relatively low temperature. It is evident from Fig. 5 that, even in the presence of slow-sintering YSZ nanoparticles, the differential sintering of the thin film electrolyte cannot be avoided due to the inherent nature of extremely fast sintering of the ultrafine precursor powder derived from chemical solution. The degree of differential densification may be reduced by increasing the content of slow-sintering YSZ nanoparticles below the critical volume fraction where they do not form local clusters.

In order to eliminate the large elongated pores, another attempt has been made to further reduce the degree of differential sintering by reducing the heating rate from 1 °C/min to 0.25 °C/min to 1100 °C. Fig. 6 shows TEM micrographs of the thin film YSZ electrolyte layers prepared by multiple spin coating of 5 vol% YSZ nanoparticle dispersed solution. Although there were still laterally elongated large pores in the thin film electrolyte layer prepared at heating rate of 1 °C/min (Fig. 6(a)), reducing heating rate to 0.25 °C/min (Fig. 6(b)) was indeed effective for decreasing the residual porosity and pore anisotropy

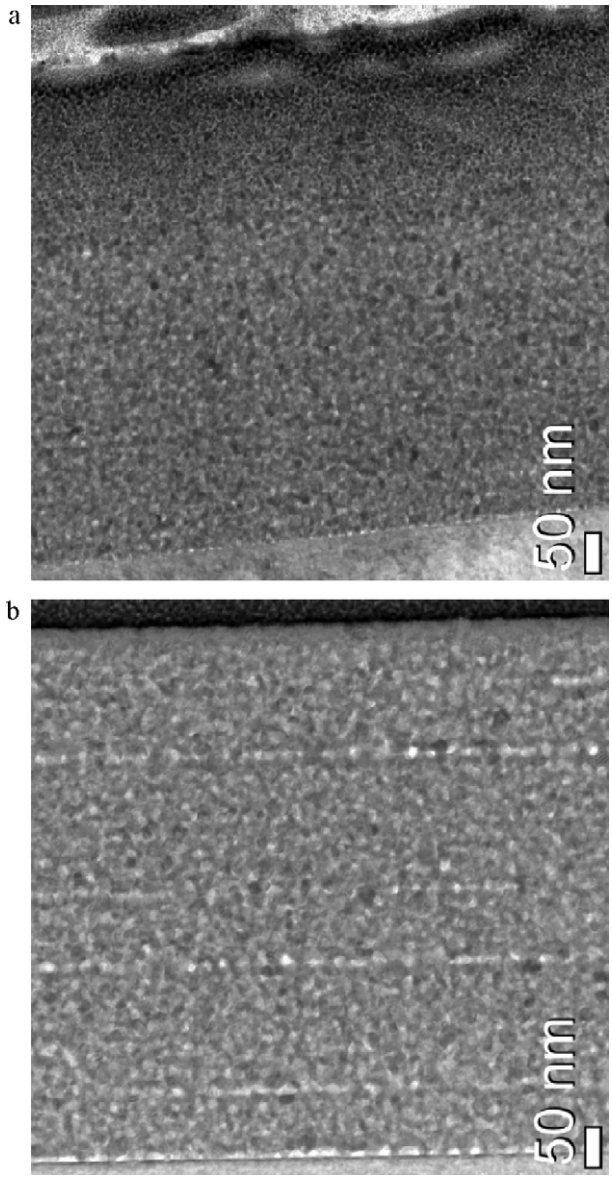

Fig. 5. TEM micrographs of the YSZ thin film electrolyte layers prepared by multiple spin coating followed by (a) resistive sintering at 800 °C and (b) microwave sintering at 800 °C.

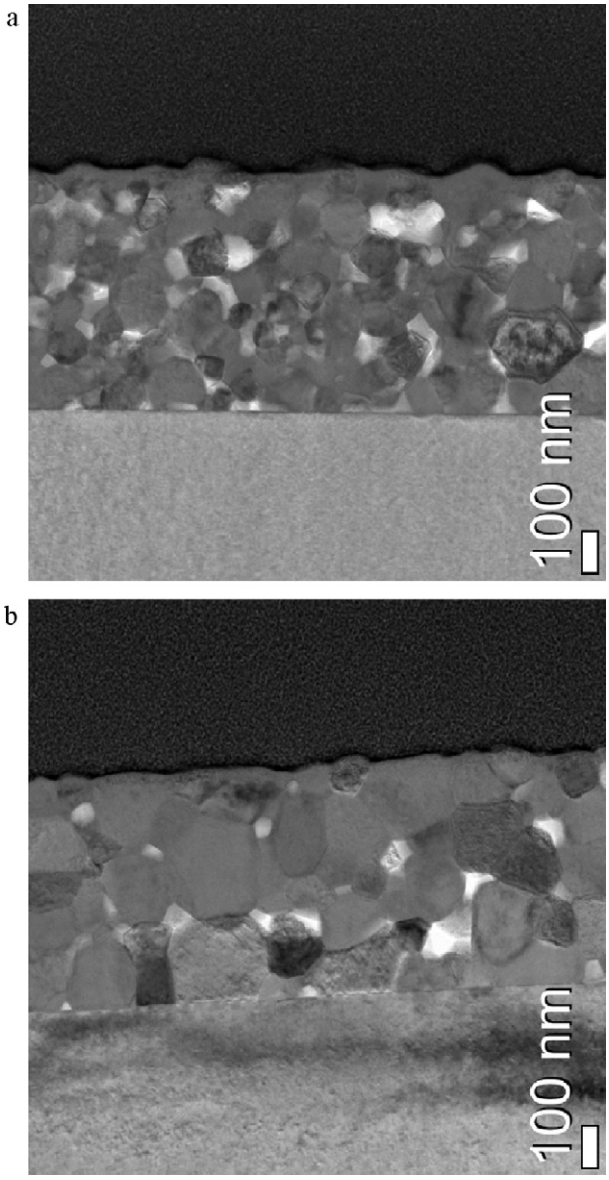

Fig. 6. TEM images of the thin film YSZ electrolyte layers sintered at 1100 °C with different heating rates: (a) 1 °C/min and (b) 0.25 °C/min.

by suppressing the differential densification. In fact, the residual porosity decreased from 9 to 5.6% and the pores became relatively equiaxed in shape with considerably reduced size. Although the grain size increased from below 100 to about 200 nm, it is still smaller than the film thickness of 500 nm, securing the structural stability against the film breakup.[7,26]

As the thin film YSZ electrolyte in this study can be sintered to relatively high density with residual pores in isolated state without major process flaws, it is worthwhile to test this thin film as an electrolyte in an actual cell architecture. A cell was fabricated by depositing a thin film electrolyte layer on a conventionally processed anode substrate and subsequently placing both GDC interdiffusion barrier and LSC cathode by PLD process.[27,28] Fig. 7 shows SEM micrographs of the surface of anode functional layer used for electrolyte coating, in which the average grain intercept size is about 0.4 μm. Since the anode substrate is actually a bilayer composite consisting of coarse-grained anode support and fine-grained anode functional layer, the surface quality in Fig. 7(a) and (b) represents the anode functional layer. Despite substrate warpage and surface roughness, the thin film electrolyte layer in Fig. 8(a) shows a smooth and dense surface without any surface cracks. It is also verified in the cross section view in Fig. 8(b) that the thin film electrolyte develops strong adhesion to the substrate without delamination cracks and the film thickness is very uniform throughout the sample in the range 400–500 nm.

Fig. 9 shows the plots of cell voltage and power density as a function of current density measured at 450–600 °C for a cell containing a thin film YSZ electrolyte by multiple spin coating of chemical solution prepared as described above. The open circuit voltage was about 1.07 V, indicating that the YSZ

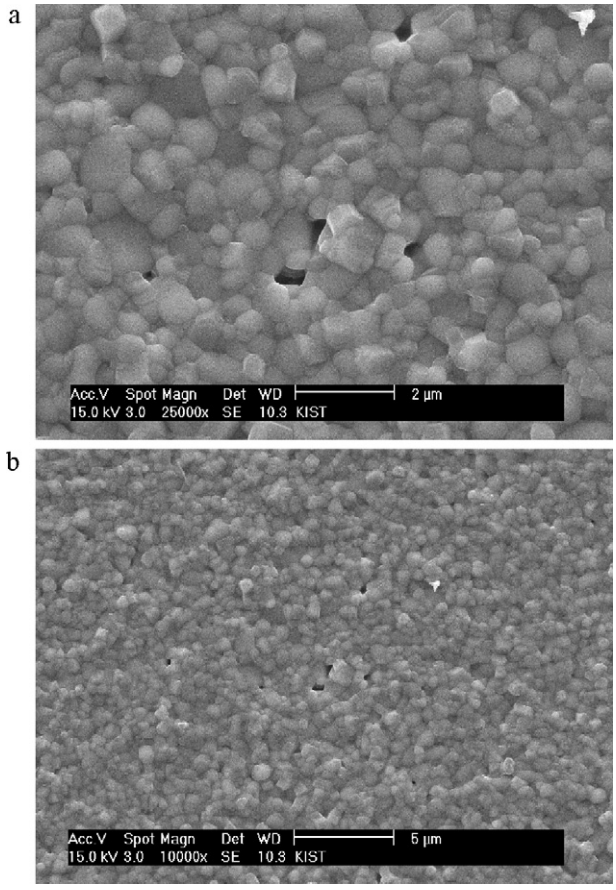

Fig. 7. SEM micrographs of the surface of anode functional layer at: (a) high magnification and (b) low magnification.

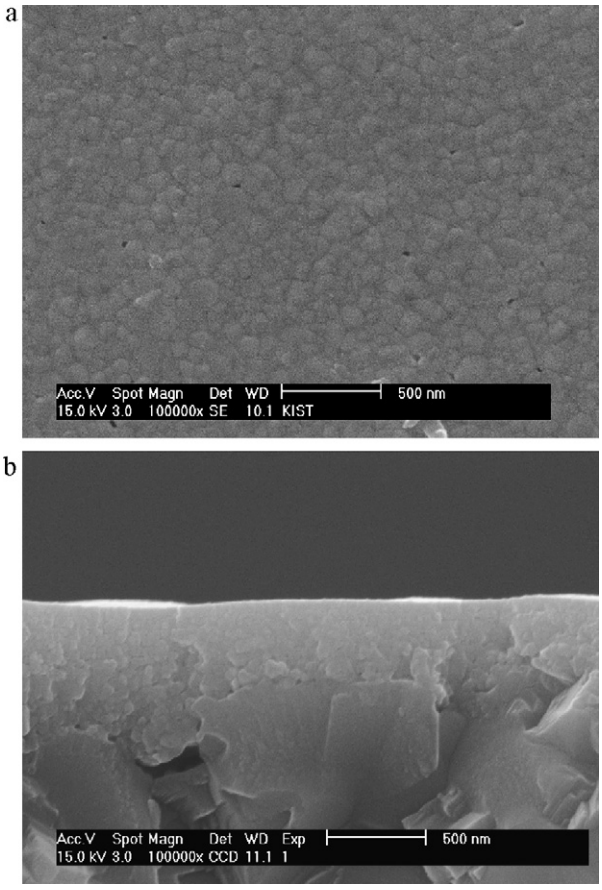

Fig. 8. SEM micrographs of the thin films YSZ electrolytes prepared by chemical solution deposition: (a) surface view and (b) cross-section view.

thin film electrolyte by chemical solution deposition has good gas tightness although it has residual porosity and its thickness is substantially reduced. The open circuit voltage obtained in this study is comparable to or better than those of the previous investigations which prepared thin film YSZ electrolytes by chemical solution deposition methods such as spin coating and spray pyrolysis.[15,29] Chen and Wei[29] did not clearly describe whether the YSZ thin film was co-fired with a green anode tape or post-fired on a sintered anode, but the good adhesion of thin film YSZ electrolyte to the anode suggests that it is co-fired at 1300 °C. The resulting YSZ electrolyte had an OCV of about 1.06 V with average grain size of 0.6 μm for the 0.5 μm thick thin film layer, which is not favorable for its structural stability against film breakup.[7,26] On the other hand, Perednis and Gaukler[15] reported that the highest OCV obtained for a 1 μm thick YSZ electrolyte prepared by ESD was 0.88 V mainly due to the incomplete coalescence of solution droplets on the surface of the substrate. To the best of our knowledge, the OCV obtained in this study is one of the highest for the thin film YSZ electrolyte obtained by chemical solution deposition on a rigid substrate. The cell with thin film YSZ electrolyte in the present study resulted in a maximum power density of 425 mW/cm^2 at 600 °C, which is also comparable to or slightly lower than those of Chen and Wei's cell with Pt/Pd cathode, e.g. 477 mW/cm^2 at 600 °C [29] and Perednis and Gaukler's cell with 50 μm thick LSCF cathode, e.g. 320–760 mW/cm^2 at 700–770 °C.[15]

Finally, SEM observation of the tested cell in Fig. 10 clearly verifies that the thin film YSZ electrolyte prepared by chemical solution deposition can successfully maintain its structural integrity with strong adhesion to the neighboring component

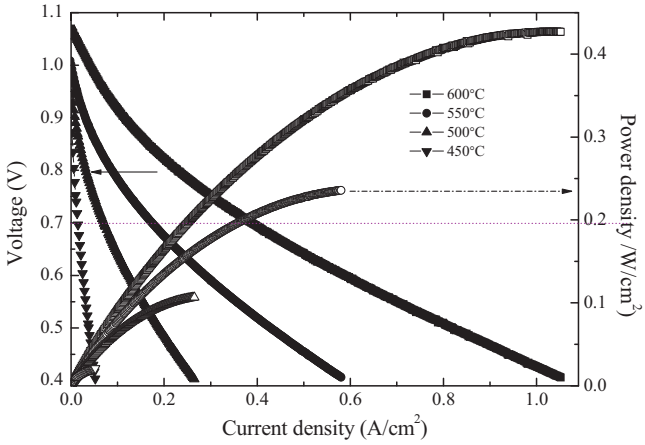

Fig. 9. Plots of cell voltage and power density as a function of current density measure at 450–600 °C for a cell containing thin film YSZ electrolyte prepared by chemical solution deposition with GDC interdiffusion barrier and LSCF cathode layers deposited by PLD process.

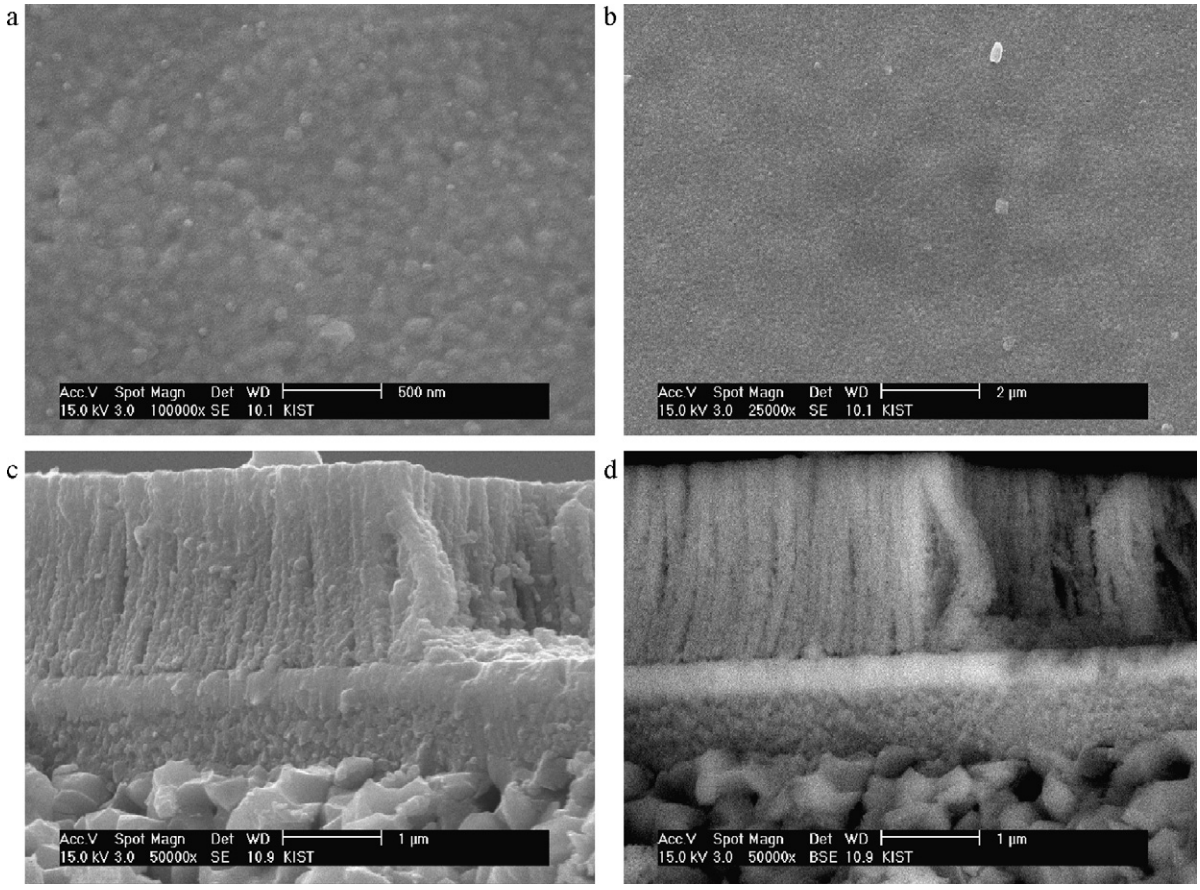

Fig. 10. SEM images of the cell containing a thin film YSZ electrolyte after cell test: (a) surface view at high magnification, (b) surface view at low magnification, (c) cross-section view at secondary electrons (SE) image and (d) cross-section view at backscattered electrons (BSE) image.

layers throughout fabrication as well as operation. Even in the presence of some surface irregularities of the substrate such as surface roughness and surface pores, the thin film electrolyte layer conformably covers the substrate surface with a relatively uniform thickness of about 400–500 nm. The thin film electrolyte layer also appears to be strongly adhered to the YSZ grains in the anode substrate, which persistently withstand the thermal stresses associated with anode reduction. Judging from the structural stability of thin film YSZ electrolyte throughout both fabrication and operation steps, it is solidly demonstrated that chemical solution route is a practical way to produce a gastight thin film YSZ electrolyte as it can be fabricated by post-firing on a sintered anode substrate rather than co-firing with an anode layer.

4. Conclusions

A thin film YSZ electrolyte of about 400–500 nm thickness was successfully produced on a conventionally processed anode substrate of non-sintering by multiple spin coating of chemical solution and sintering at low temperature with substantially reduced microstructural heterogeneity and pore anisotropy. Constrained sintering and differential densification were effectively suppressed by incorporating 5 vol% slow-sintering YSZ nanoparticles with the particle size of about 20 nm, which could mitigate the prevailing bi-axial constraint of the rigid substrate with the numerous local multi-axial stress fields around them. The thin film YSZ electrolyte placed on a rigid anode substrate with the GDC and LSC layers deposited by PLD process revealed that it had fairly good gas tightness relevant to a SOFC electrolyte and maintained its structural integrity during fabrication and operation processes. In fact, the open circuit voltage was 1.07 V and maximum power density was 425 mV at 600 °C, which are very comparable to the reported values for the cells containing thin film electrolyte prepared by chemical solution route. This study clearly demonstrates that the chemical solution deposition can be applied to produce a gastight and ultrathin electrolyte even on a rigid substrate, which makes it possible to optimize the microstructures and functions of individual layers by a layer-by-layer construction.

Acknowledgments

This work was supported by the Institutional Research Program of the Korea Institute of Science and Technology (KIST) and the Fundamental R&D Program for Core Technology of Materials funded by the Ministry of Knowledge Economy, Republic of Korea.

References

1. Kueper T, Visco S, De Jonghe L. Thin-film ceramic electrolytes deposited on porous and non-porous substrates by sol–gel techniques. *Solid State Ionics* 1992;**52**:251–9.
2. De Jonghe L, Jacobson C, Visco S. Supported electrolyte thin film synthesis of solid oxide fuel cells. *Annu Rev Mater Res* 2003;**33**:169–82.
3. Zhu Q, Fan B. Low temperature sintering of 8YSZ electrolyte film for intermediate temperature solid oxide fuel cells. *Solid State Ionics* 2005;**176**:889–94.
4. Chourashiya MG, Bharadwaj SR, Jadhav LD. Synthesis and characterization of electrolyte-grade 10% Gd-doped ceria thin film/ceramic substrate structures for solid oxide fuel cells. *Thin Solid Films* 2010;**519**:650–7.
5. Pan Y, Zhu J, Hu M, Payzant E. Processing of YSZ thin films on dense and porous substrates. *Surf Coat Technol* 2005;**200**:1242–7.
6. Gestel TV, Sebold D, Meulenberg WA, Buchkremer HP. Development of thin-film nano-structured electrolyte layers for application in anode-supported solid oxide fuel cells. *Solid State Ionics* 2008;**179**: 428–37.
7. Butz B, Stormer H, Gerthsen D, Bockmeyer M, Kruger R, Ivers-Tiffe E, et al. Microstructure of nanocrystalline yttria-doped zirconia thin films obtained by sol–gel processing. *J Am Ceram Soc* 2008;**91**:2281–9.
8. Lin H, Ding C, Sato K, Sutai T, Hashida T. Low-temperature anode-supported SOFC with ultra-thin ceria-based electrolytes prepared by modified sol–gel route. *J Solid Mech Mater Eng* 2010;**4**:335–44.
9. Ding C, Lin H, Sato K, Hashida T. A simple, rapid spray method for preparing anode-supported solid oxide fuel cells with GDC electrolyte thin films. *J Membr Sci* 2010;**350**:1–4.
10. Wang D, Wang J, He C, Tao Y, Xu C, Wang WG. Preparation of a $Gd_{0.1}Ce_{0.9}O_{2-d}$ interlayer for intermediate-temperature solid oxide fuel cells by spray coating. *J Alloy Compd* 2010;**505**:118–24.
11. Martinez-Amesti A, Larranage A, Rodrituez-Martinez LM, Aguaty AT, Pizarro JL, Arriortua MI. Reactivity between $La(Sr)FeO_3$ cathode, doped CeO_2 interlayer and yttria-stabilized zirconia electrolyte for solid oxide fuel cell applications. *J Power Sources* 2008;**185**:401–10.
12. Hui R, Wang Z, Yick S, Maric R, Ghosh D. Fabrication of ceramic films for solid oxide fuel cells via slurry spin coating technique. *J Power Sources* 2007;**172**:840–4.
13. Petrovsky V, Suzuki T, Jasinski P, Petrovsky T, Anderson H. Low-temperature processing of thin-film electrolyte for electrochemical devices. *Electrochem Solid-State Lett* 2004;**7**:A138–9.
14. Rose L, Kesler O, Tang Z, Burgess A. Application of sol gel spin coated yttria-stabilized zirconia layers for the improvement of solid oxide fuel cell electrolytes produced by atmospheric plasma spraying. *J Power Sources* 2007;**167**:340–8.
15. Perednis D, Gauckler LJ. Solid oxide fuel cells with electrolytes prepared via spray pyrolysis. *Solid State Ionics* 2004;**166**:229–39.
16. Wang Z, Sun K, Shen S, Zhou X, Qiao J, Zhang N. Effect of co-sintering temperature on the performance of SOFC with YSZ electrolyte thin films fabricated by dip-coating method. *J Solid State Electrochem* 2010;**14**:637–42.
17. Lin H, Ding C, Sato K, Tsutai Y, Ohtaki H, Iguchi M, et al. Preparation of SDC electrolyte thin films on dense and porous substrates by modified sol–gel route. *Mat Sci Eng B* 2008;**148**:73–6.
18. Tomov R, Krauz M, Jewulski J, Hopkins S, Kluczowski J, Glowacka D, et al. Direct ceramic inkjet printing of yttria-stabilized zirconia electrolyte layers for anode-supported solid oxide fuel cells. *J Power Sources* 2010;**195**:7160–7.
19. Diaz-Parralejo, Caruso R, Ortiz A, Guiberteau F. Densification and porosity evaluation of ZrO_2–3 mol% Y_2O_3 sol–gel thin films. *Thin Solid Films* 2004;**458**:92–7.
20. Teixeira EC, Piascik JR, Stoner BR, Thompson JY. Effect of YSZ thin film coating thickness on the strength of a ceramic substrate. *J Biomed Mater Res B: Appl Biomater* 2007;**83B**:459–63.
21. Malzbender J, Fischer W, Steinbrech RW. Studies of residual stresses in planar solid oxide fuel cells. *J Power Sources* 2008;**182**:594–8.
22. Cheon JH, Shankar PS, Singh JP. Influence of processing methods on residual stress evolution in coated conductors. *Supercon Sci Technol* 2005;**18**:142–6.
23. Wright GJ, Yeomans JA. Constrained sintering of yttria-stabilized zirconia electrolytes: the influence of two-step sintering profiles on microstructure and gas permeance. *Int J Appl Ceram Technol* 2008;**5**:589–96.
24. Liu HK, Azar PM. Effect of particle addition on drying stresses and the green density of sol–gel processed three-dimensional ceramic-matrix composites. *J Am Ceram Soc* 1998;**81**:1824–8.
25. Jung HY, Choi SH, Kim H, Son JW, Kim J, Lee HW, et al. Fabrication and performance evaluation of 3-cell SOFC stack based on planar 10 cm × 10 cm anode-supported cells. *J Power Sources* 2006;**159**:478–83.
26. Miller KT, Lange FF, Marshall DB. The instability of polycrystalline thin films: experiment and theory. *J Mater Res* 1990;**5**:151–60.
27. Noh HS, Lee HO, Kim BK, Lee HW, Lee JH, Son JW. Microstructural factors of electrodes affecting the performance of anode-supported thin film yttria-stabilized zirconia electrolyte (∼1 μm) solid oxide fuel cells. *J Power Sources* 2011;**196**:7169–74.
28. Noh HS, Lee HO, Ji HI, Lee HW, Lee JH, Son JW. Limitation of thickness increment of lanthanum strontium cobaltite cathode fabricated by pulsed laser deposition. *J Electrochem Soc* 2011;**158**:B1–4.
29. Chen YY, Wei WC. Processing and characterization of ultra-thin yttria-stabilized zirconia (YSZ) electrolytic films for SOFC. *Solid State Ionics* 2006;**177**:351–7.